ORIGINAL ARTICLE

Analytical model for prediction of bend angle in laser forming of sheets

Sujit Mulay[1] · Vineet Paliwal[1] · N. Ramesh Babu[1]

Abstract
This paper covers an analytical approach for predicting the bend angle of a laser formed sheet with a single laser scan. The proposed approach is based on the strain energy stored under the laser-irradiated area that causes plastic deformation of sheet due to laser heating. With any particular intensity of laser, the temperature profile established across the sheet thickness is determined by employing a one-dimensional transient heat conduction equation and by considering the loss of heat to the surrounding material by thermal conduction. Based on the temperature gradient across the sheet thickness, thermal strain, strain-induced stress, and bending moment are evaluated. By equating the strain energy stored in the sheet material due to thermal stress and strain with the strain energy stored due to the bending moment, the angle of bend in the sheet is determined. The results obtained with the proposed model are validated with the experiments performed on AISI 304 stainless steel and AA 1100 aluminum alloy sheet material of different thickness using CO_2 laser with varying power and scanning speed. A three-dimensional finite element model is developed to validate the temperature profile predicted by the proposed model. The effectiveness of the proposed approach is validated by comparing the predicted bend angle with those predicted by other analytical models. Apart from this, the effect of various process parameters on the laser formed sheet was studied using microstructure and microhardness analysis. Finally, with the application of the proposed model, a process map is generated to achieve pure bending during laser forming.

Keywords Laser forming · Bending angle · Analytical model · Strain energy theory

1 Introduction

Laser forming is a non-contact method of forming metallic sheets with the induction of thermal stresses by controlled laser heating of sheets. This method has several benefits such as high flexibility, negligible spring-back, absence of external tooling, and the ability to form complex profiles [1, 2]. Due to these benefits, this method has received significant attention in aerospace, shipbuilding, and microelectronics industries for straight-line bending, rapid prototyping, shape correction, and micro-scale adjustments [3]. It is a complex thermo-mechanical process, influenced by various process parameters such as laser power, scanning speed, beam shape and size, thermal and mechanical properties of sheet material, and

geometrical parameters of the sheet [4, 5]. To automate the laser forming process for commercial applications, it becomes essential to study the effect of these parameters on the bend angle. Attempts were made to study the influence of various process parameters on bend angle during laser forming of different sheet materials using techniques such as numerical [6–10], empirical [11–13], analytical [14–21], and soft computing [22, 23] modeling.

The earliest work on laser forming by Geiger and Vollertsen [24] suggested three different mechanisms such as thermal gradient mechanism (TGM), buckling mechanism (BM), and upsetting mechanism (UM), based on the specific combinations of laser parameters and sheet parameters. Vollertsen [25] proposed an analytical model to predict the bend angle of the laser formed sheet by elastic bending theory. The model is computationally efficient and describes the effect of main process parameters on the bend angle. However, the model overpredicts the bend angle due to several assumptions like temperature gradient is a step function, the effect of thermal conductivity is negligible, and the strain induced in the heated layer is fully converted into plastic strain and

✉ N. Ramesh Babu
nrbabu@iitm.ac.in

[1] Manufacturing Engineering Section, Department of Mechanical Engineering, Indian Institute of Technology Madras, Chennai 600036, India

neglected the effect of elastic properties of sheet material. A similar approach used by Yau et al. [26] considered the counter bending effect, which includes the elastic properties of the sheet material. It is a composite approach with two equations, first for estimating the bend angle after cooling stage and the second for estimating the counter bending angle during laser heating. Cheng and Lin [27] proposed three artificial neural network (ANN)–based models to estimate the bend angle: (1) Back-propagation neural network (BPNN) with hyperbolic tangent function, (2) BPNN with logistic function, and (3) radial basis neural network (RBFN) and found that RBFN model predicts accurate bend angle than former approaches. Kyrsanidi et al. [15] developed a parametric model for predicting the bend angle of a plate based on TGM, wherein the thermal strain induced during the heating stage was considered to estimate the final bend angle. Cheng et al. [16] derived a formula for bend angle by considering the pre-bending effect of consecutive segments along the laser scan path for finite sheet width and length.

All these models predict the bend angle considering TGM with a steep temperature gradient. Hence, the prediction accuracy of such models will be poor for a gradual temperature gradient due to the co-existence of TGM and BM. Shen et al. [17] derived an expression for bend angle based on a history-dependent incremental stress-strain relationship, suitable for both the phenomenon of TGM and BM. Lambiase [18] developed a closed-form analytical model based on Vollertsen's two-layer approach. In this model, heated layer thickness was determined based on temperature drop along with the sheet thickness. Although the model shows accurate results for low conductive materials, it gives inaccurate results for highly conductive materials, as it ignores the heat loss due to conduction into the surrounding material. An improved model, considering the heat loss due to conduction into the surrounding material, was proposed by Lambiase and Ilio [19] whereby the energy loss due to heat conduction was calculated using regression analysis and was assumed to be fixed. However, the model shows inaccurate results for thin sheets of highly conductive material processed with low scanning speed.

In recent times, artificial neural network and finite element–based models were developed to predict the bend angle. Lambiase et al. [23] proposed an ANN-based model to optimize the processing time required to achieve the desired bend angle. Fetene et al. [22] developed ANN model based on the FEM data to estimate the bend angle of a preloaded sheet. Navarrete and Celentano [10] used a FE-based model to investigate the effect of scanning strategies on the deformation of different sheet geometries to realize complex shapes using laser forming. Although ANN-based models are easy to develop, the reliability of these models depends upon the training dataset collected from experiments or other models. FE-based models predict accurate bend angle and provide insight into the process. However, FE-based models are computationally expensive and the accuracy of such models depends on several factors such as coupling of thermal and mechanical behavior of the process, selection of mesh size, etc. On the other hand, analytical models are found to be computationally efficient over FEM and ANN models, as these models do not require any pre-simulations and experiments.

Most of the existing analytical models [18, 19, 25, 26] predict bend angle by considering a fraction of the total sheet thickness, which is heated effectively. Generally, this heated sheet thickness is estimated by measuring the thermal penetration depth for a given laser intensity. As the thermal penetration depth depends on several factors such as optical, thermal, mechanical, and geometrical attributes of the sheet, an accurate prediction of thermal penetration depth becomes challenging. The certainty of these models is highly dependent on the accuracy of the estimation of the heat-affected sheet thickness. Therefore, it is required to select a parameter that is simple to estimate and can directly be related to the bend angle formed during laser forming. Thermal stress and strain are the two parameters that are directly related to the final bend angle. Therefore, average strain energy across the sheet thickness, estimated by the combination of thermal stress and strain, can be correlated with the final bend angle.

In the present work, an analytical model is proposed based on the strain energy stored beneath the laser-irradiated area that causes plastic deformation of sheet. A one-dimensional transient heat conduction equation is used to evaluate the temperature profile across the sheet thickness. For accurate estimation of the temperature profile, the heat loss due to conduction to the surrounding material is determined by the application of the finite difference method. Based on the temperature distribution, the thermal stress, thermal strain, and bending moment are evaluated. By equating the strain energy stored in the sheet material due to thermal stress and strain to that needed for bending moment, the bend angle of the sheet is determined. A series of experiments were performed using a continuous wave CO_2 laser on AISI 304 stainless steel and AA 1100 aluminum alloy sheets. A 3D FEM is developed to validate the temperature distribution across the sheet thickness predicted by the proposed model. The accuracy of the proposed model is confirmed by comparing the predicted bend angle with the experimentally measured bend angle and also with the published results. A good correlation is observed between the proposed model and the experimental results for both of the sheet materials processed under wide operating conditions. Apart from this, the effect of process parameters on the laser formed sheet was studied using microstructure and microhardness analysis. Finally, with the application of the

proposed model, a process map is generated to achieve pure bending during laser forming.

2 Methodology

When a metal sheet is irradiated by laser beam along the sheet surface, a non-uniform temperature profile develops across the sheet thickness, which in turn induces thermal strains in the irradiated area and forces the surrounding material to react. The reaction of the surrounding material to resist thermal strain results in thermal stresses. As these thermal stresses exceed the yield strength of sheet material, it deforms the sheet material plastically. As laser forming involves the interaction of several process parameters that affect the thermomechanical phenomenon of the process. It becomes important to consider all these properties while developing an analytical model to predict the bending angle accurately. Figure 1. shows the schematic of a straight-line laser forming process.

The following assumptions were made in developing the model and are based on the practical condition of laser forming:

i.   Heat flux distribution across the cross-section of the beam is uniform.
ii. The temperature rise in the laser-irradiated area does not cause any surface melting.
iii. The gravitational force on the sheet is neglected.
iv. Phase transitions are not considered.
v.   Creep strains are neglected.
vi. Plastic deformation across the laser scanning path is uniform; i.e., edge effect is neglected.

The development of the model is attempted in two parts. The first part deals with thermal modeling that covers the estimation of non-uniform temperature profile across the sheet thickness. The second part deals with the prediction of thermal stresses and strains induced across the thickness of sheet and the resultant bend angle. Figure 2 shows the methodology adopted for the development of the proposed model.

2.1 Thermal modeling

For determining the temperature profile across the sheet thickness, the following assumptions are made: The sheet material is isotropic and homogeneous and its thermal and mechanical properties are considered to be independent of temperature. The heat loss due to convection and radiation is also considered negligible.

Therefore, the temperature profile across the sheet thickness is estimated using a one-dimensional transient heat conduction and considering the sheet as a semi-infinite thick sheet.

$$\frac{\partial^2 T(s,t)}{\partial s^2} = \frac{1}{\alpha}\frac{\partial T(s,t)}{\partial t} \tag{1}$$

Here, 'α' is thermal diffusivity of sheet material given as $\alpha = k/\rho C_p$, 's' is the thickness of sheet in mm, 'ρ' is the density of sheet material in kg/m^3, 'C_p' is the specific heat capacity in J/kgK, 'T' is the temperature in °C, and 'k' is the thermal conductivity in W/mK of the sheet material.

By applying initial and boundary conditions, the temperature profile across the sheet thickness can be determined with Eq. (2) [14, 25].

$$\Delta T_{\text{initial}}(s) = T_0 + \frac{6.92AP}{\pi d^2 k}\left\{\left(\sqrt{\alpha t_i}\right)ierfc\left[\frac{s}{2\sqrt{\alpha t_i}}\right]\right\} \tag{2}$$

Here, 'A' is the laser absorptivity, 'P' is the laser power in Watt, 'd' is the laser beam diameter in mm, 'T_o' is the ambient temperature in °C, 't_i' is the laser interaction time with the sheet in second, calculated by considering the unit width of the sheet $t_i = 1/v$, 'v' is the laser scanning speed along the sheet width in mm/s, and '$ierfc$' is the integral of the complementary error function.

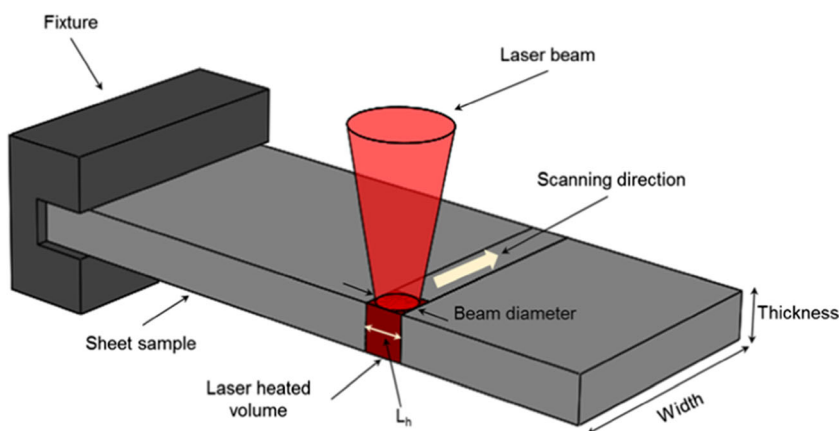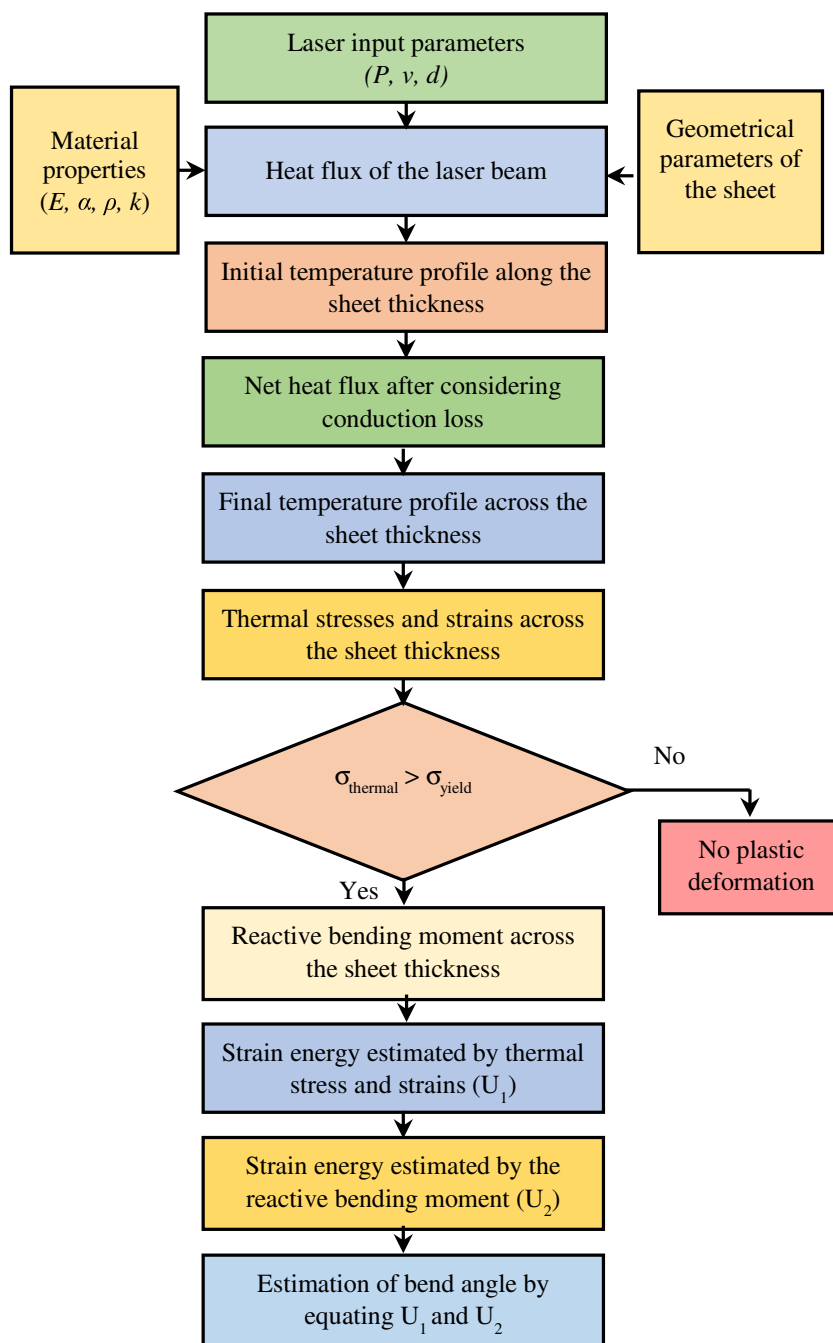**Fig. 1** Schematic representation of straight-line laser forming process

Fig. 2 Methodology followed for the development of the proposed analytical model

However, the loss of heat due to thermal conduction from laser-heated area to the surrounding material needs to be considered for accurate estimation of temperature profile across the sheet thickness [19]. Figure 3 shows the steps followed for determining the final temperature profile across the sheet thickness considering the loss of heat due to conduction into the surrounding material.

For estimating the heat loss, Eq. (3) derived from the finite difference method is used [26]. First, the initial temperature profile determined with Eq. (2) is used to estimate the mean temperature across the sheet thickness using Eq. (4). The same

mean temperature was considered to determine the loss of heat due to conduction.

$$Q_{loss} = Q_{input} + ks\left\{\frac{T_o - 2T_{mean} + T_o}{\Delta y^2}\right\} \tag{3}$$

$$T_{mean} = \frac{\sum_{i=1}^{n} T_i}{n} \tag{4}$$

Here, 'Q_{input}' is the heat flux supplied to the sheet by laser beam in J, 's' is the sheet thickness in mm, and 'T_{mean}' is the mean temperature across the sheet thickness °C. 'Δy' is the
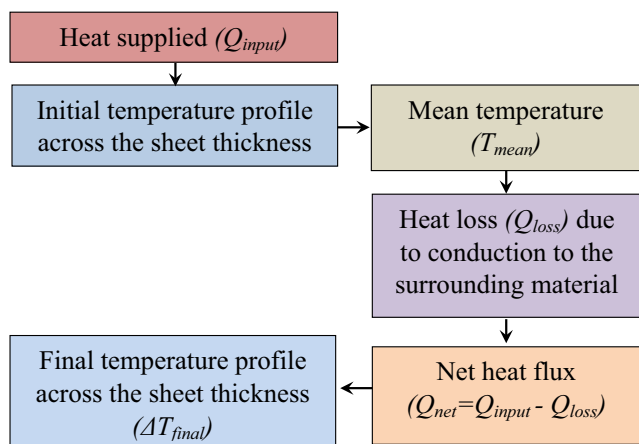
Fig. 3 Steps followed for determining the final temperature profile across the sheet thickness
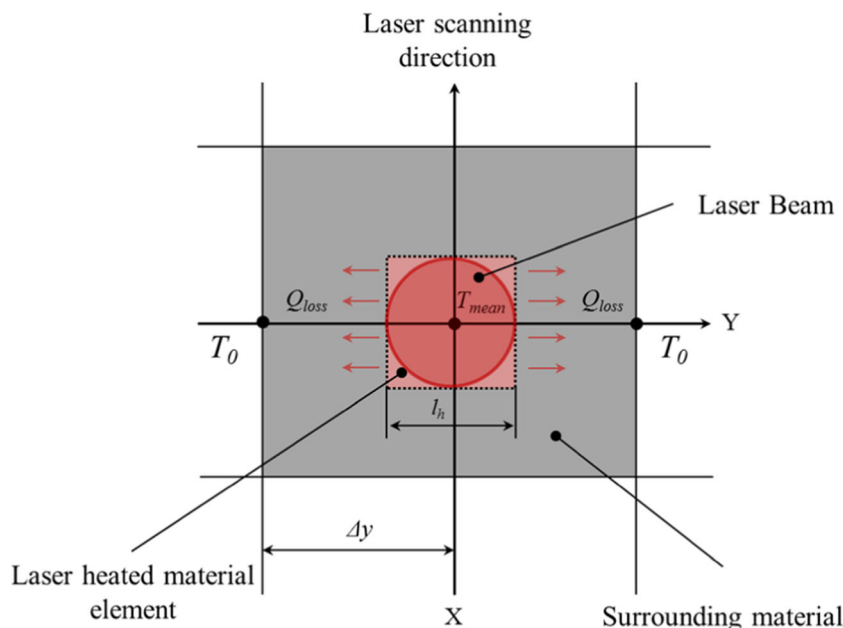
distance between the central node and the node at which the temperature has dropped to ambient temperature. Figure 4 shows the temperature nodes considered for determination of the heat loss along the top sheet surface. For AISI 304, it is considered $1.5_{/h}$, and for AA1100, it is considered $2l_h$; 'l_h' is the heated length in mm.

A heat loss factor (β) is calculated by taking the ratio of Q_{loss} to Q_{input}, and using the same in Eq. (2), the final temperature profile across the sheet thickness was predicted by Eq. (5).

$$\Delta T_{final}(s) = T_0 + \beta \frac{6.92AP}{\pi d^2 k} \left\{ \left(\sqrt{\alpha t_i}\right) ierfc \left[\frac{s}{2\sqrt{\alpha t_i}}\right] \right\} \quad (5)$$

In the next section, thermal stresses and strains across the sheet thickness are estimated based on the final temperature profile obtained from Eq. (5).

2.2 Mechanical modeling

In this step, the average strain energy stored in laser-heated volume due to the generation of thermal stresses, thermal strains, and bending moment is evaluated. To determine the thermal stresses and strains, the mean temperature across the sheet thickness is considered based on the final temperature profile using Eq. (5). Figure 5 shows the thermal stress distribution and bending moment along the laser-irradiated area.

The resulting longitudinal thermal stresses and strains across the sheet thickness are determined by using Eqs. (6) and (7) respectively.

$$\sigma_{th} = \alpha_{th} E(\Delta T_{final}(s)) \quad (6)$$

$$\varepsilon_{th} = \alpha_{th}(\Delta T_{final}(s)) \quad (7)$$

Here, 'α_{th}' is the coefficient of linear thermal expansion and 'E' is Young's modulus of elasticity.

The average strain energy stored in laser-heated volume due to thermal stresses and strains across the sheet thickness is given as,

$$U\sigma, \varepsilon, \text{average} = \frac{1}{2}\sigma_{th,average}\varepsilon_{th,average}V \quad (8)$$

Here, 'V' is the heated volume for unit width is given by Eq. (9).

$$V = l_h s \quad (9)$$

Similarly, the strain energy stored due to reactive bending moment is estimated by using the eq. (10).

$$U_{bending\ moment} = \frac{1}{2}Md\theta \quad (10)$$

Fig. 4 Heat loss due to conduction along the top sheet surface (i.e., longitudinal direction) from laser-irradiated area

Fig. 5 Thermal stress distribution and bending moment along the laser-irradiated area
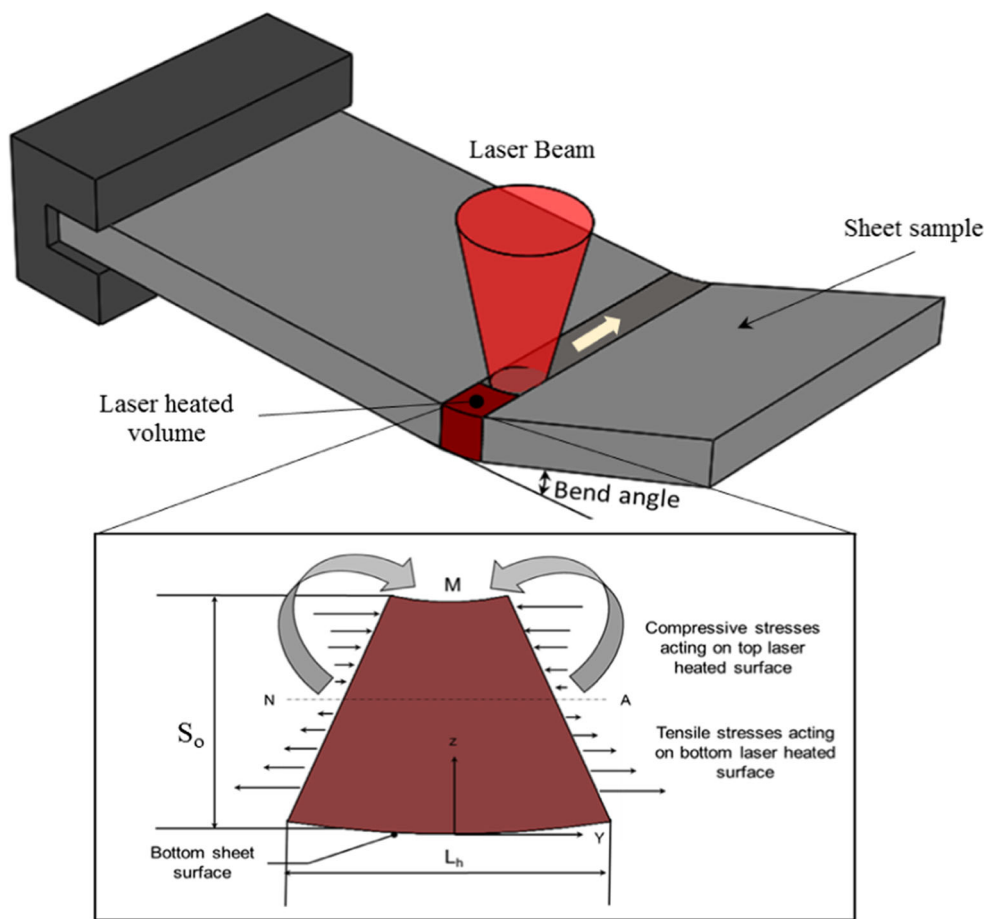
Here, 'M' is the bending moment determined from Eq. (11).

$$M = \frac{EI}{l_h} d\theta \qquad (11)$$

Here, 'I' is the moment of inertia of the sheet and is given as,

$$I = \frac{1}{12} l_h s^3 \qquad (12)$$

Here, 'l_h' is the laser-heated length and 's' is the sheet thickness.

Finally, the bend angle induced in the sheet is determined from Eq. (13) derived by equating Eq. (8) and Eq. (10).

$$d\theta = \frac{\sigma_{th} \varepsilon_{th} V}{M} \qquad (13)$$

2.3 Finite element modeling

A three-dimensional finite element model was developed using commercial software COMSOL MULTIPHYSICS v 5.2, to estimate the temperature distributions across the sheet thickness for different laser processing conditions. The assumptions made in the model are as follows: the heat loss due to conduction is considered in the model. However, convection and radiation losses are neglected. The von Mises criterion is considered a yielding criterion, and the dissipation of energy during plastic deformation was ignored. A laser beam with heat flux (Q) is applied over the sheet surface. The temperature profile across sheet thickness is estimated by using Fourier heat conduction, as given in Eq. (1). A three-dimensional tetrahedral shape of elements with 0.6 mm length is selected for the meshing of the 3-D model.

3 Experimental setup and procedure

An experimental setup for laser forming is shown in Fig. 6. Laser forming setup comprises of a laser source, beam delivery system, sheet clamping unit, and control system. A continuous wave CO_2 laser (AMADA, Quattro), with a maximum power of 1 kW emitted at a wavelength of 10.6 μm, is used to perform the experimental tests.

For the sample preparation, the sheet samples of AISI 304 stainless steel material were cut in the dimensions of 100 mm ×

Fig. 6 Experimental setup used for the laser forming of sheet
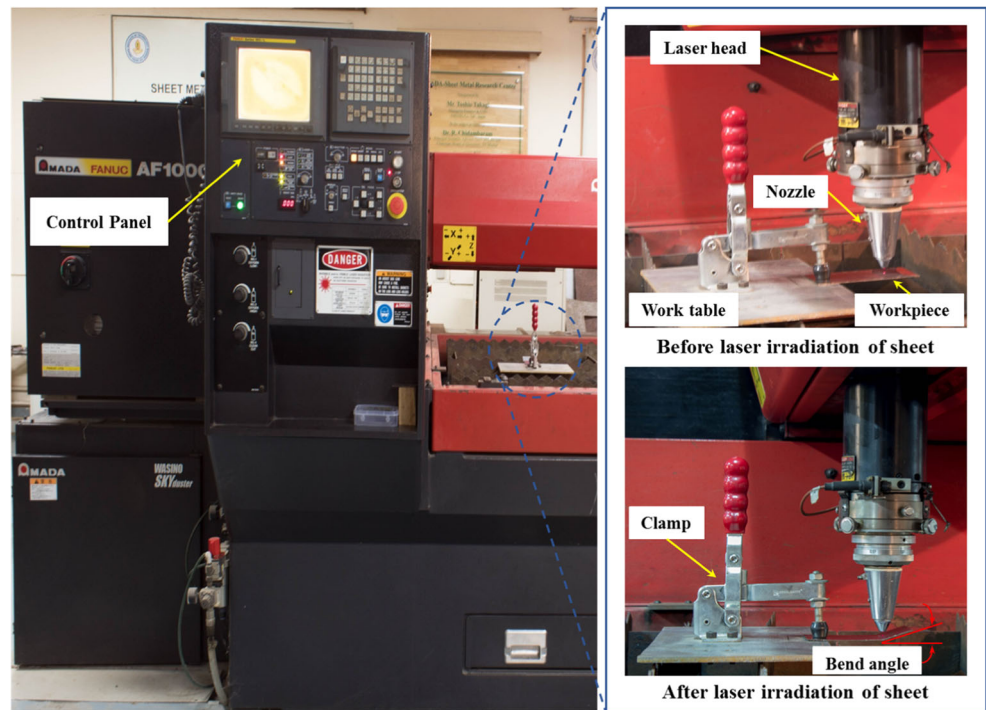
50 mm × 2 mm and 100 mm × 50 mm × 1 mm and the sheet samples of AA1100 were cut in the dimensions of 100 mm × 50 mm × 1 mm. Table 1 shows the thermal and mechanical properties of AISI 304 stainless steel and AA 1100 sheet material. The sheet surface was cleaned using acetone to remove the surface impurities and then coated with the graphite powder (graphite 33) and cured at a temperature of 215 °C for 30 min in order to increase the absorption of the laser beam. The absorption coefficient for both AISI 304 and AA 1100 sheet material was considered 0.6 [16, 27]. The coated sheet sample was clamped at one end using a toggle clamp and is free at the other end. A laser beam of 1.5 mm diameter was focused on the top surface of the sheet and is moved along the sheet width.

Experiments were performed by choosing the different combinations of laser power and scanning speeds for two different thicknesses of sheet, as shown in Table 2. For each sheet thickness, totally, nine experiments were performed with the choice of different laser parameters. After each experiment, the bend angle induced in a single laser scan was measured using a non-contact coordinate measuring machine. Figure 7a shows the CMM setup used for measuring the bend angle. Three readings were taken at three different locations, i.e. start, middle, and end, along the sheet width and the average value of the bend angle was considered as the final bend angle. The experimental temperature was measured using a k-type thermocouple (range of − 200 to 1260 °C), which was fixed to the bottom of the sheet surface and the temperature was recorded using a data acquisition system, as shown in Fig. 7b. To study the effect of laser parameters on the microstructural changes on sheet samples due to laser heating, the irradiated area on the sample was analyzed using the scanning electron microscope (SEM) images. For this purpose, the samples were first polished using silicon carbide emery sheets of different grades (600–3000 grit size) and then subjected to velvet polishing with 1 μm size of a particle of diamond paste. The polished specimens were etched with Glyceregia etchant for 90 s. Microhardness of the bent zone, across the sheet thickness, was measured using a Vickers microhardness tester by applying an indentation load of 300 g for 10 s.

Table 1 Thermal and physical properties of sheet material

Materials	Properties				
	ρ (kg m^{-3})	C_p (J kg^{-1} K^{-1})	k (W m^{-1} K^{-1})	α_{th} (K^{-1})	E (N m^{-2})
AISI 304	7850	500	19	17×10^{-6}	210×10^{9}
AA 1100	2710	904	222	23.6×10^{-6}	69×10^{9}

Table 2 Range of parameters used for experimental tests

Material	Sheet thickness (mm)	Laser power (W)	Scanning speed (mm/min)
AISI 304	1.0	200	900
	2.0	300	1200
		400	1500
AA1100	1.0	200	900
		300	1200
		400	1500

4 Results and discussion

In this section, the results predicted by the proposed model are compared with the experimental results, FE model results, and the results predicted by the models proposed by Vollertsen [28] and Lambiase [18]. The accuracy of the proposed model is assessed by comparing the results predicted with the proposed model for two different types of materials of 1-mm and 2-mm thickness and is processed by employing different combinations of laser parameters, shown in Table 2.

4.1 Validation of temperature distribution

The temperature profile predicted with the proposed model is compared with the results obtained by the FE model. Figure 8 a and b show the temperature distribution across the sheet thickness estimated by the proposed analytical model and FE-based model for AISI 304 steel sheet, respectively. From these results, it can be observed that the temperature field predicted by the proposed analytical model is in good agreement with the temperature predicted with the FE-based model. Figure 8c shows the temperature profile for AA1100 alloy sheet across the sheet thickness considering the heat loss and without heat loss. A considerable variation in the temperature profile predicted with both the conditions can be observed, which can affect the prediction accuracy of the final bend

angle. The experimental temperature results induced in the single laser scan are measured using the k-type thermocouple. It was observed that the bottom sheet surface temperature remained the same as the room temperature for AISI 304 steel sheet. Similar temperature results are predicted by the proposed analytical model, as shown in Fig. 7a.

4.2 Validation of the bend angle

The proposed model is compared with the experimental results and also with the results given by Vollertsen [25] and Lambiase [18] models. Figures 9 and 10 show the comparison of predicted bend angle for the AISI 304 steel sheet of thickness 1 mm and 2 mm respectively, processed with different laser power and scanning speed. From these results, it can be observed that the proposed model predicted the bend angle accurately for both thin as well as thick sheets. It can also be observed that the bend angle induced in the sheet has decreased at higher scanning speeds. The main reason for this particular trend in bend angle variation can be attributed to the reduction in the interaction time of the laser beam with the sheet surface. This sort of trend is observed with both thicknesses of the sheet. However, the results predicted with the Lambiase model did not follow this trend, especially with thin sheets of 1-mm thickness. Furthermore, it can be noticed that the accuracy of results predicted with the proposed model is higher at low laser power compared with that predicted with higher laser power (Fig. 9). The proposed model predicted the bend angle with an accuracy of 89.73% at 200 W, whereas the accuracy of prediction is found to be 83.47% at 400 W for a sheet of 1 mm thick. This discrepancy in prediction can be attributed to the strain hardening of laser-heated area at higher laser power.

The accuracy of the proposed model is assessed by comparing the bend angle predicted for AA1100 aluminum alloy sheet material, i.e., highly conductive material of 1 mm thickness processed with different laser parameters. Figure 11

Fig. 7 Experimental measurements. **a** CMM setup used for the bend angle measurement. **b** Temperature measurement setup

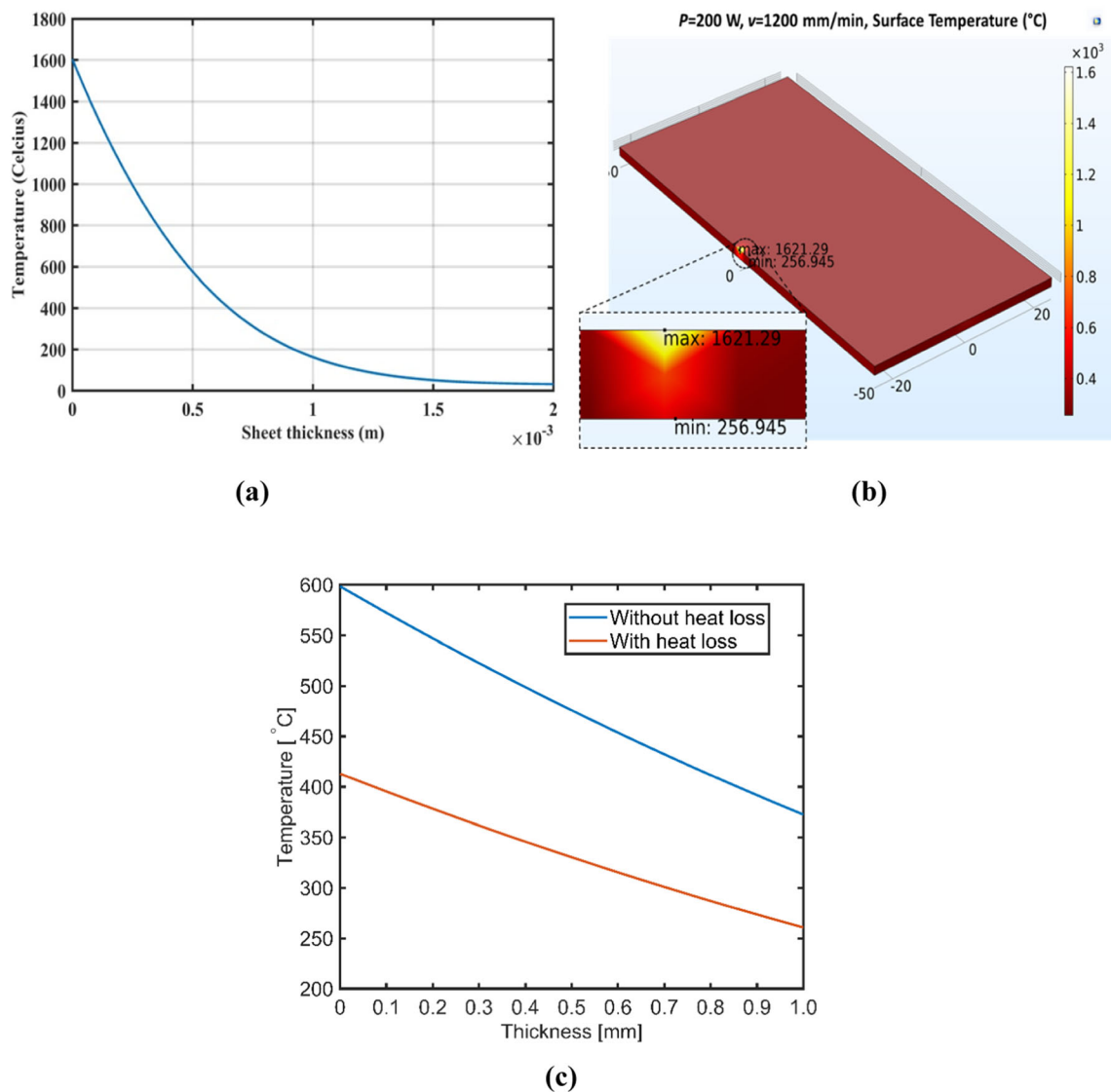**(a)**   **(b)**

(a)

(b)

(c)
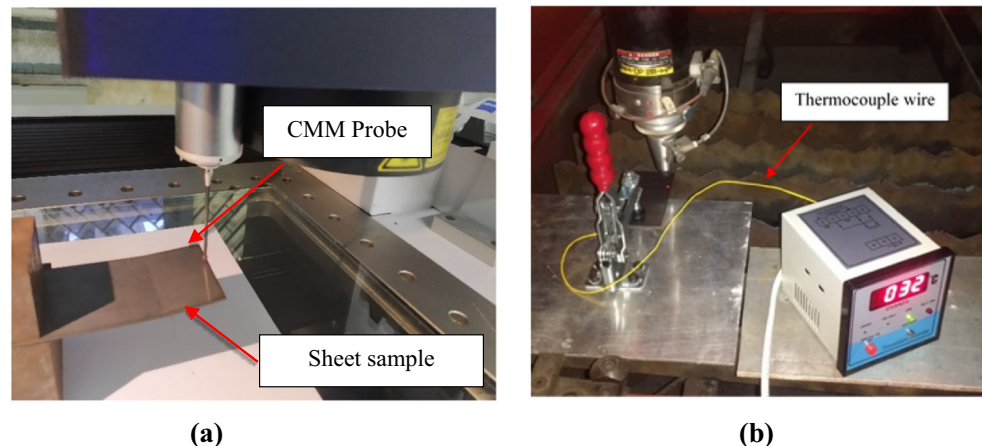
Fig. 8 Temperature distribution along the sheet thickness. a Final temperature profile predicted by the proposed model after considering the heat loss. b Temperature distributions predicted by the FE-based model for AISI 304 steel. c Temperature profile for AA1100 along the thickness with and without heat loss due to conduction (P = 200 W, v = 1200 mm/min, d = 1.5 mm)

shows the comparison of predicted bend angle with the experimental bend angle. It can be observed that the proposed model results are significantly improved for AA 1100 alloy sheet material over the results predicted with Vollertsen and Lambiase model. One of the major reasons for the higher accuracy of prediction of results, for high conductive materials, with the proposed model compared with the results with other models could be due to the consideration of thermal stress and strain induced across the sheet thickness.

By comparing the results obtained with the proposed model and the results of experimental work for AISI 304 steel sheet and AA 1100 aluminum sheet, it can be observed that the bend angle values of AISI 304 steel sheet vary significantly with different laser power and scanning speed. At the same time, for AA 1100 aluminum sheet, the bend angle is almost

uniform irrespective of the laser power and the scanning speed. The variation in bend angle for both of the sheet materials could be due to the difference in their thermal conductivities. During laser heating, the loss of heat due to thermal conduction into the surrounding material is much higher for AA 1100 sheet when compared with that conducted into AISI 304 steel sheet material. Therefore, for accurate prediction of the bend angle for highly conductive materials, it is necessary to consider the loss of heat by conduction into the surrounding material.

Tables 3 and 4 show the average error, and the maximum error noticed for AISI 304 SS of 1-mm and 2-mm thickness respectively. The present model is found to predict the bend angle more accurately with an average error of 13.06% and a maximum error of 32.98% for a 1-mm-thick sheet. In contrast

Fig. 9 Comparison of experimental results and published model results with the predicted bend angle result. **a** AISI 304 steel sheet of 1-mm thickness (P = 200 W). **b** AISI 304 steel sheet of 1-mm thickness (P = 300 W)



(a)   (b)
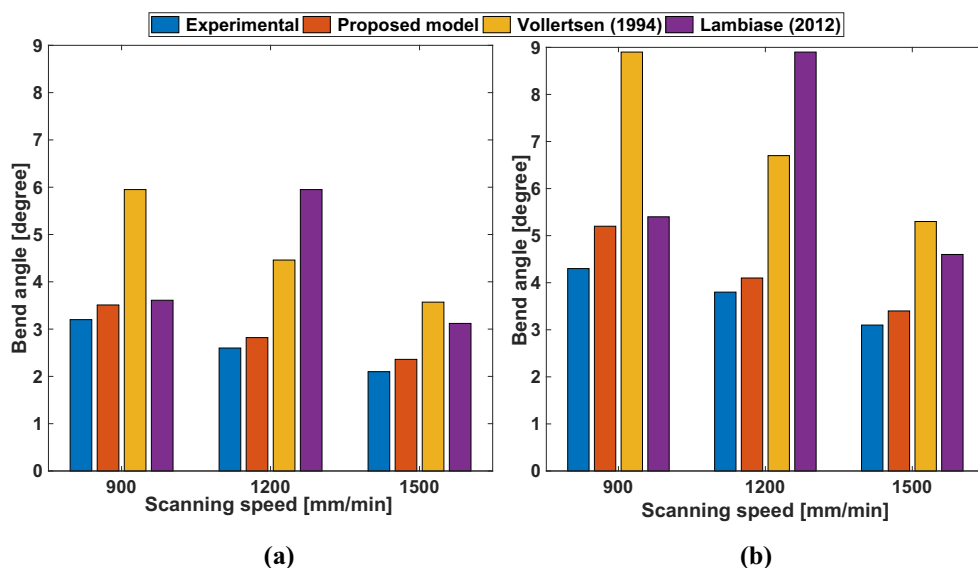
to this, for a 2-mm-thick sheet, the average error was 8.20% and a maximum error of 16.19% for the proposed model. With the proposed model, a significant improvement in the prediction of bend angle of sheets processed with a wide operating range is observed when compared to the predicted results with other models. This improvement in prediction accuracy can be attributed to the application of a novel strain energy–based approach in this model development. One of the major discrepancies noticed with the existing models [18, 19, 25, 26] is that those models considered only fraction of sheet thickness as laser heat affected, based on the thermal penetration depth by the laser beam. However, the thermal penetration depth depends on several factors such as optical, thermal, mechanical, and geometrical attributes. Therefore, the certainty of these models is highly dependent on the accuracy of the

estimation of the heat-affected sheet thickness. Contrastingly, the proposed model made it simple to estimate parameters such as thermal stress, thermal strain, and bending moment which are in turn used to estimate the bend angle.

4.3 Effect of processing parameters on the laser formed sheet

In the present section, the effect of processing parameters such as laser power, scanning speed, and number of scans on the different aspects of the laser formed sheet are discussed (Fig. 12). The related variation of thermal stress and strain and its effect on the strain energy is also explained in detail. The microstructure and microhardness obtained in different zones of the laser-irradiated area, i.e., across the sheet

Fig. 10 Comparison of experimental results and published model results with the predicted bend angle result. **a** AISI 304 steel sheet of 2-mm thickness (P = 200 W). **b** AISI 304 steel sheet of 2-mm thickness (P = 400 W)
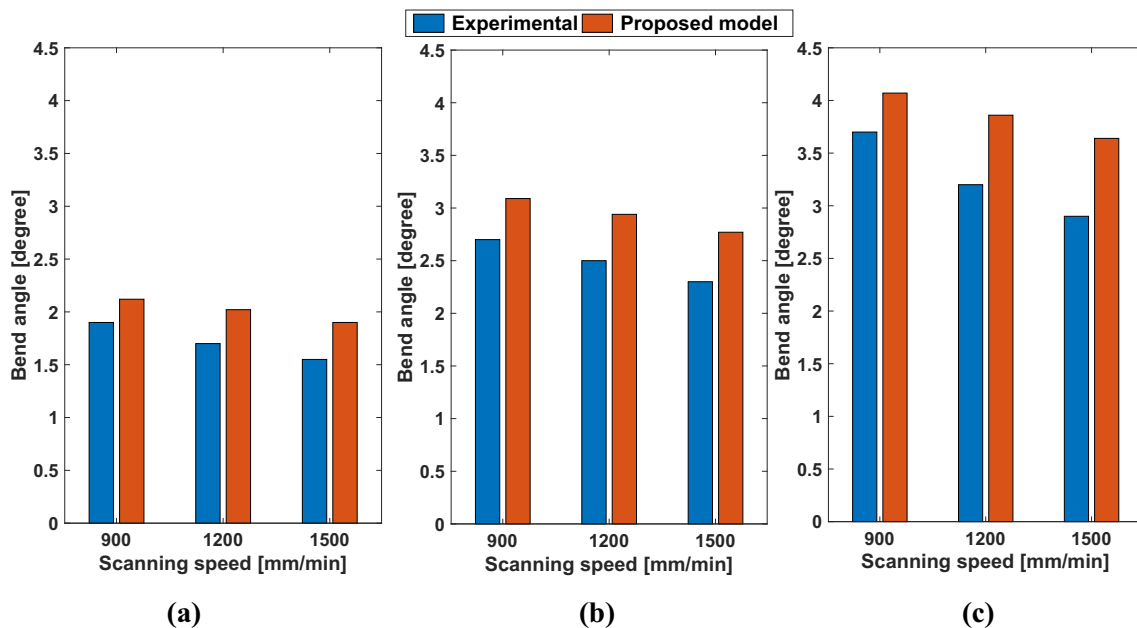

(a)   (b)
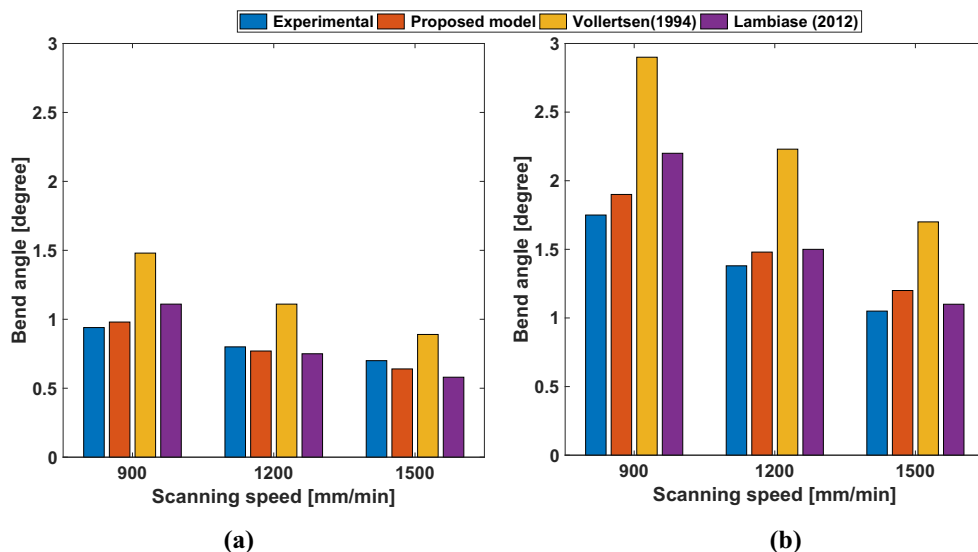
Fig. 11 Comparison of experimental result with the proposed model result for AA 1100 sheet of 1-mm thickness for **a** $P = 200$ W, **b** $P = 300$ W, and **c** $P = 400$ W

thickness, are analyzed and correlated with the process parameters. Finally, with the application of a proposed model, a process map is generated to achieve a defect-free bend during laser forming.

4.3.1 Effect of process parameters on the bend angle

Figure 13 shows the laser formed sheet samples processed with different laser parameters. From the results presented in these figures, it can be seen that the bend angle increased with an increase in the number of scans with the constant line energy, i.e., energy input per unit length (P/V). With an increased in the number of scans, the energy supplied to the sheet surface has increased, which in turn has resulted in an increase in the magnitude of deformation.

The variation in the bend angle with respect to the input laser power was also studied. In Fig. 13 c and d, it can be seen that the bend angle has increased with an increase in laser power. In fact, the scanning speed and the number of scans were kept constant while the laser power was doubled. But the bend angle has not increased in proportion to laser power. This

non-uniform variation of sheet deformation can be attributed to several interrelated factors such as geometrical effects, variation in thermal and physical properties of the sheet material with respect to temperature, and microstructural variation.

4.3.2 Stress and strain distribution

Thermal stresses and strains depend on the temperature profile over the sheet during laser forming, which in turn depend on the values of laser parameters such as laser power, scanning speed, beam diameter, and the number of scans. Due to localized heating, a thermal expansion of the sheet takes place. This expansion is resisted by the surrounding material of the sheet. As a result of this, thermal stresses are developed across the thickness of the sheet. With different settings of these laser parameters, different thermal profiles will be generated which are responsible for the variation of thermal stresses and strains in laser-irradiated sheet. Tables 5 and 6 show the variation of average stress and strain with respect to laser power and scanning speed for AISI 304 steel sheet of thickness 1 mm and 2 mm, respectively. It can be observed that for a constant

Table 3 Prediction accuracy of the proposed model for AISI 304 steel sheet of thickness 1 mm

	Proposed model	Vollertsen model [25]	Lambiase model [18]
Average error (%)	13.06	78.67	56.55
Maximum error (%)	32.98	129.07	153.33

Table 4 Prediction accuracy of the proposed model for AISI 304 steel sheet of thickness 2 mm

	Proposed model	Vollertsen model [25]	Lambiase model [18]
Average error (%)	8.20	49.10	14.16
Maximum error (%)	16.19	71.80	28.35

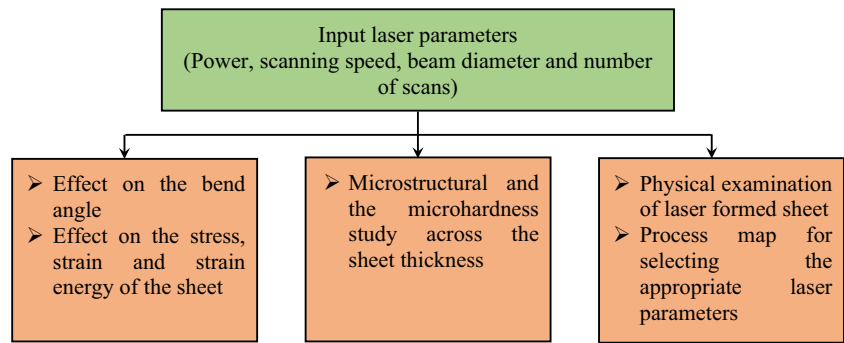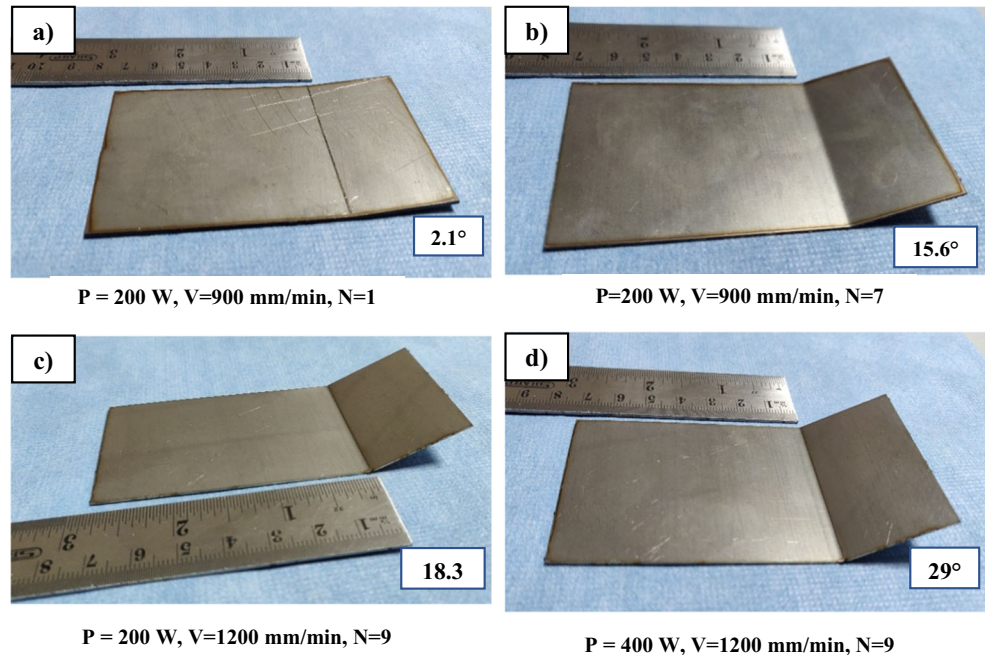**Fig. 12** Effect of input laser parameters on different aspects of laser formed sheets

Fig. 13 Laser formed AISI 304 stainless steel sheet samples processed with different input laser parameters

scanning speed, the thermal stress increases with the increase of laser power, which increases the strain energy stored in sheet and leads to higher plastic deformation. In contrast, with constant laser power, an increase in scanning speed decreases the thermal stress and also decreases the plastic deformation, as the amount of heat flux required to induce plastic strain becomes insufficient.

As the bend angle depends on the strain energy stored due to the thermal stresses and strains, it becomes important to understand the effect of laser parameters on the strain energy.

Table 5 Stress and strain variations in laser formed AISI 304 steel sheet of 1 mm thickness

Power (W)	Scanning speed (mm/min)	Average stress (MPa)	Average strain
200	900	3040	0.0145
200	1200	2444	0.0116
200	1500	2045	0.0097
300	900	4507	0.0215
300	1200	3612	0.0172
300	1500	3015	0.0144

Table 6 Stress and strain variations in laser formed AISI 304 steel sheet of 2 mm thickness

Power (W)	Scanning speed (mm/min)	Average stress (MPa)	Average strain
200	900	1695	0.0081
200	1200	1338	0.0064
200	1500	1112	0.0053
300	900	2489	0.0119
300	1200	1954	0.0093
300	1500	1614	0.0077

Fig. 14 Effect of laser parameters on strain energy. **a** For AISI 304 SS of 1-mm thickness. **b** For AISI 304 SS of 2-mm thickness. **c** For AA 1100 of 1-mm thickness
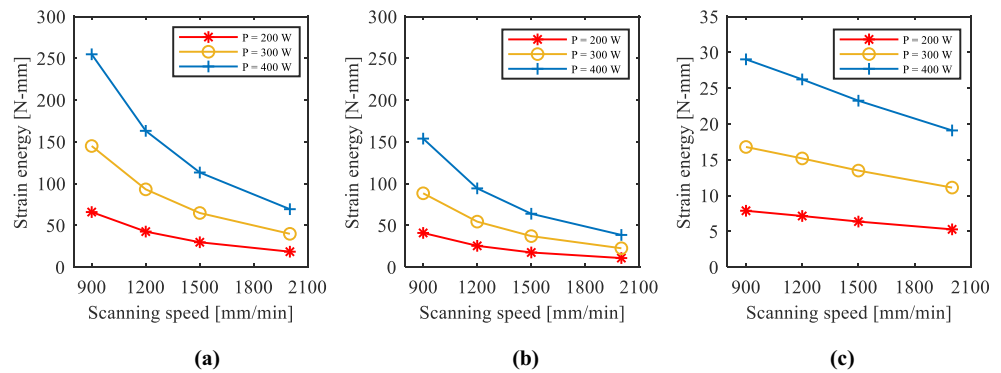

Figure 14 shows the variation in the strain energy for AISI 304 SS and AA 1100 sheet material with different laser power and scanning speed. It can be observed that the trend followed by the strain energy is almost similar to the bend angle. Figure 14(a) and Fig. 14(b) show the variation of strain energy for AISI 304 SS for 1 mm and 2 mm sheet thickness respectively. From Fig. 14a, it can be noticed that for the same laser power, the energy stored in the 1 mm-thick sheet is higher compared with that in the 2 mm sheet, which leads to the higher plastic deformation of 1 mm sheet. It can also be observed that at low scanning speed, the increment in strain energy is very high with respect to laser power, whereas, at higher scanning speed, the change in strain energy is small. Figure 14c shows the variation of strain energy stored in AA1100 sheet for different combinations of laser parameters. From this figure, it can be observed that for a constant scanning speed, the effect of increasing the laser power is highly significant for the AA1100 sheet. In contrast, the effect of the increase in scanning speed on strain energy stored is less significant.

4.3.3 Microstructural study

Microstructure evolved during the laser forming of AISI 304 steel sheet was analyzed using the scanning electron microscope (SEM) and is correlated with the process parameters. From Fig. 15a–f, variation in the microstructure across the sheet thickness is observed, as the temperature distribution across the sheet thickness is non-uniform. Microstructure across the sheet thickness is divided into four different regions based on the grain size and its orientation, namely (i) re-solidified zone, (ii) equiaxed fine-grain zone, (iii) transition zone, and (iv) heat-affected zone. A re-solidified zone up to a depth of 10 μm is observed in the proximity of the laser-irradiated surface (Fig. 15b). In this zone, the grains are found to be diffused because of rapid heating and cooling after each laser scan. Because of the diffused grains, no proper grain orientation is observed, and this is the reason that the hardness value in this particular zone is very low. The depth of this re-

solidified zone is found to be increasing with the increase of input heat flux. In the subsequent zone, fine equiaxed grains with a size of approximately 2 μm are observed (Fig. 15c). The sufficient amount of cooling rate is the main reason for the formation of these equiaxed fine grains in this zone. Because of grain refinement, a comparatively higher value of microhardness is observed in this particular zone. The next zone after the equiaxed grain zone is the transition zone. A clear variation of microstructure can be seen in this zone (Fig. 15d). Because of plastic deformation at relatively low temperature, the elongation of grains is observed in this region. The microhardness value in this zone is relatively low compared with the equiaxed grains. The last region observed during the microstructural study is the heat-affected zone, as shown in Fig. 15e. In this zone, less variation in the microstructure is observed. However, the microhardness value is higher compared with the samples as-received. The reason for an increase in hardness in this zone can be attributed to strain hardening effect or cold working.

4.3.4 Microhardness study

Microhardness values in the laser-irradiated area (across the cross-section) are measured using a Vickers microhardness tester. Figure 16 shows the average hardness distribution across the sheet thickness of AISI 304 steel samples. The microhardness of the re-solidified zone is moderately higher (around 170 VHN) compared with the microhardness of the base metal (160 VHN). The increase in hardness in the re-solidified zone can be attributed to the loss of strength due to repeated melting and solidification of the sheet in consecutive laser scans. Following the re-solidified zone, an increase in the value of microhardness (around 230 VHN) is observed due to grain refinement. In the subsequent zone, a slightly lower value of hardness (around 210 VHN) is observed as compared to the fine-grain zone due to the grain coarsening effect. Figure 17 a and b show the effect of laser power on the microhardness value for AISI 304 steel sheets of thickness
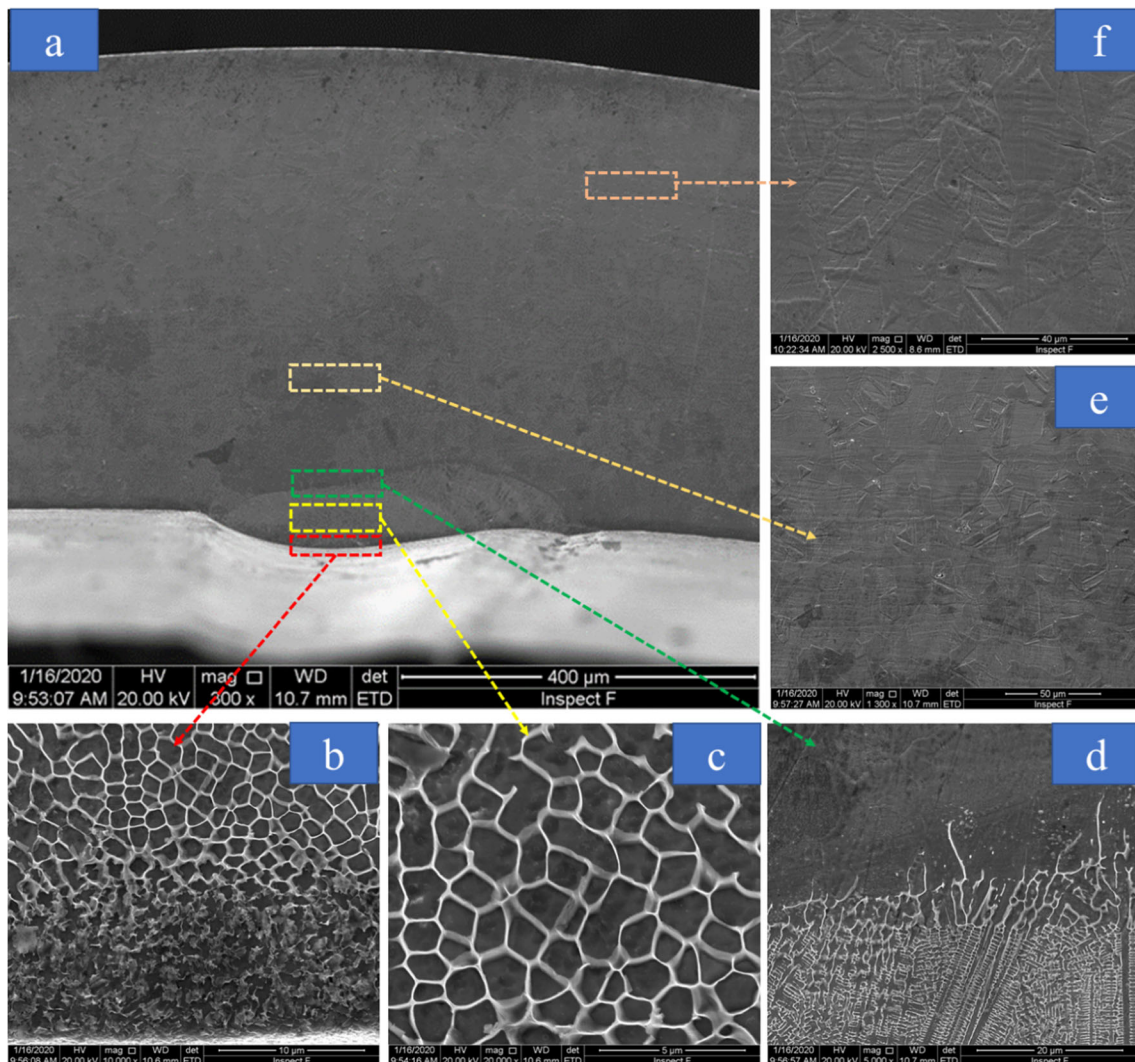
Fig. 15 Microstructure of laser formed AISI 304 steel sheet sample ($P = 200$ W, $V = 900$ mm/min, and $n = 7$)

1 mm and 2 mm, respectively. It can be observed that laser forming of the sheet, at higher laser power, causes an increase in the microhardness value, due to enlargement of the equiaxed grain zone. In the case of thin sheets, a relatively higher value of microhardness is observed compared to with thick sheets because of larger equiaxed grain zone.

5 Application of the proposed model

A process map is generated for laser forming of AISI 304 steel sheet with the application of the proposed analytical model. The process map is drawn by considering the power density ($P_{den} = 4P/\pi d^2$) and the interaction time ($t = d/V$) during laser

Fig. 16 Schematics of hardness distribution in laser-irradiated area (along the cross-section) for AISI 304 steel sheet

170 VHN
230 VHN
210 VHN
160 VHN
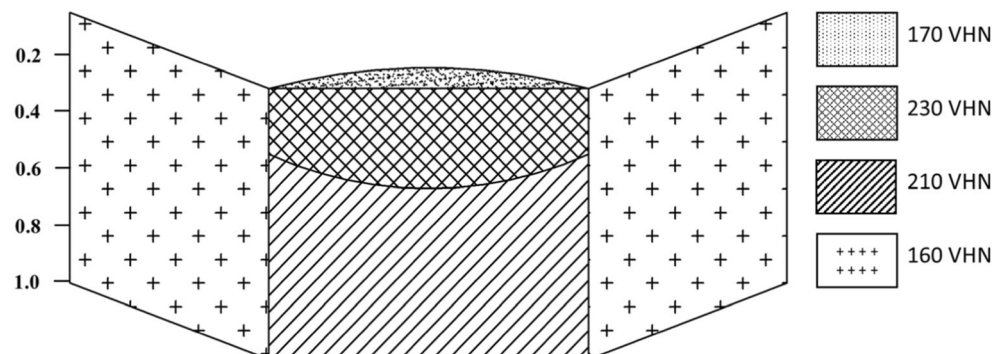
forming. Three different regions are identified based on the average temperature across the sheet thickness. These regions are classified as the pure bending region, bending + melting region, and bending + melting + cutting region. The parameters corresponding to pure bending can easily be selected by the application of this process map. For example, from Fig. 18, for pure bending of 2 mm sheet of AISI 304, the maximum power density and interaction time should be below or equal to the 226 W/mm^2 and 0.0667 s respectively. For the validation of the proposed process map, the experiments were performed, and the laser formed sheet was examined physically to investigate the bending, melting, and cutting phenomena in the laser-irradiated area. Figure 19 shows the laser formed sheet samples irradiated with two different laser parameters. With the close comparison of Fig. 19 a and b, it can be observed that the sheet sample processed with an input power of 500 W and a scanning speed of 900 mm/min finds negligible melting, whereas, in sheet sample processed with a laser power of 200 W and a scanning speed of 900 mm/min, a pure bending is observed.

Fig. 18 Process map for laser forming of AISI 304 steel sheet of thickness 2 mm

6 Conclusions

An analytical model is proposed to predict the bend angle of laser formed sheet using strain energy approach. The following are some of the major advantages of the proposed model:

- The proposed model incorporates the effect of all the important parameters such as laser parameters, material properties, and the geometrical parameters of the sheet.
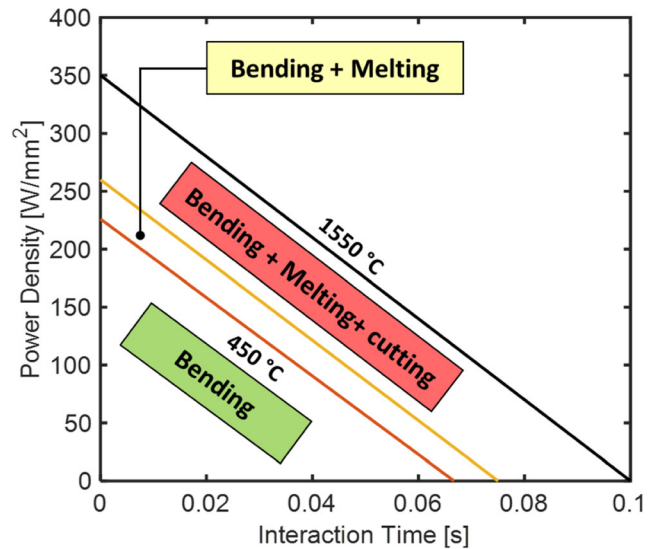- For accurate estimation of the temperature profile across the sheet thickness, heat loss due to conduction to the surrounding material is considered using a finite difference method and is validated with the finite element results.
- The proposed model is capable of predicting an accurate bend angle irrespective of the sheet thickness and its material.

The following conclusions are drawn based on the results:

i. The proposed model is validated with the experimental results for two materials, AISI 304 steel (low thermal conductivity) and AA1100 (high thermal conductivity) of different sheet thicknesses. The effectiveness of the proposed

Fig. 17 Average microhardness of AISI 304 steel along the sheet thickness processed with a scanning speed of 900 mm/min for 7 number of scans for **a** 1.0-mm and **b** 2.0-mm sheet thickness
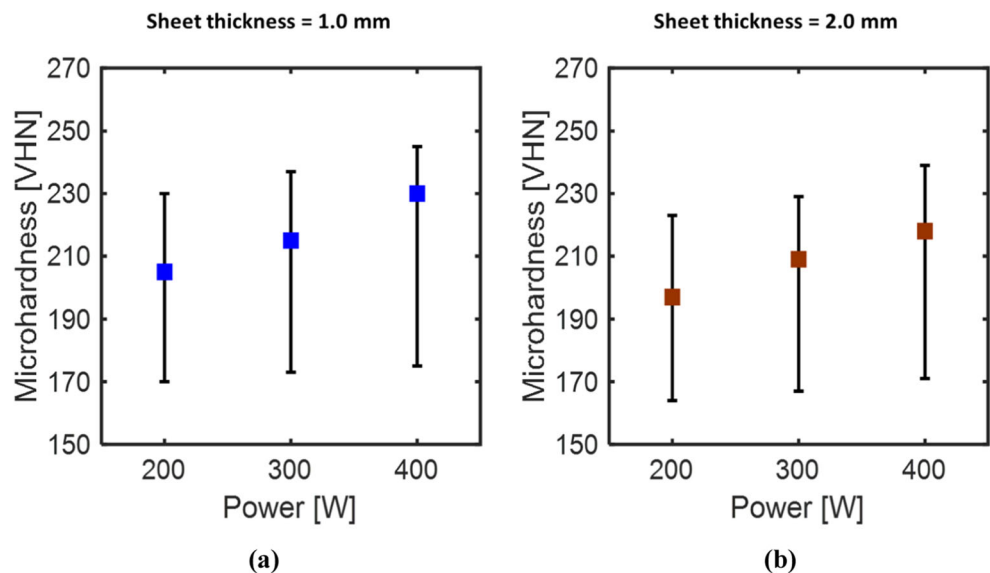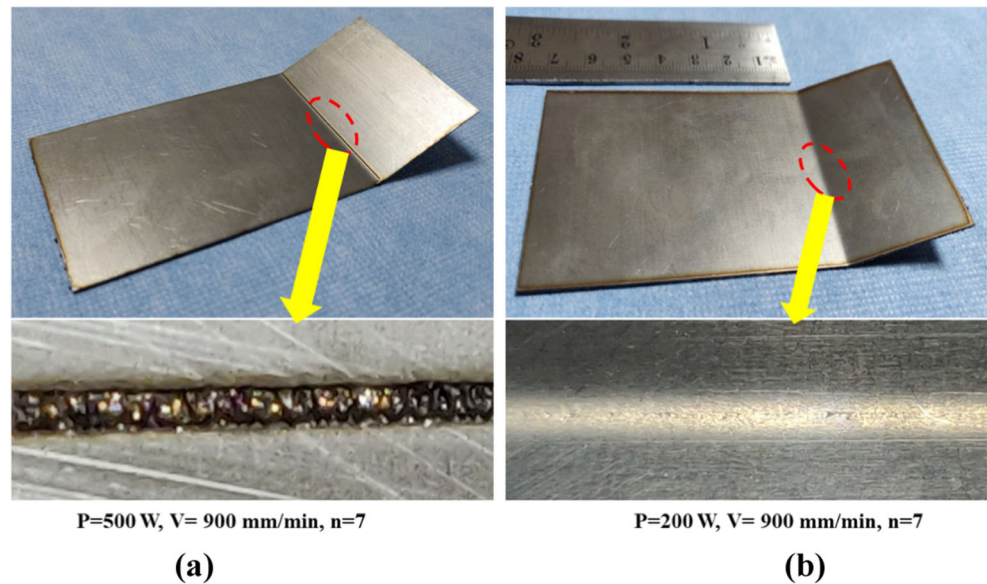

(a)

(b)

Fig. 19 Laser irradiated samples **a** with negligible melting and **b** without melting

P=500 W, V= 900 mm/min, n=7

(a)

P=200 W, V= 900 mm/min, n=7

(b)

model is also demonstrated by comparing the predicted bend angle results with published analytical models.

ii. The accuracy of the proposed model for AISI 304 steel sheet of thickness 1 mm is around 87% and for a 2 mm sheet thickness is around 92%.

iii. The microstructural analysis of laser irradiated area was performed, and four different regions (re-solidified zone, equiaxed grains, transition zone, and heat-affected zone) are identified across the sheet thickness based on the grain size and their orientation.

iv. The microhardness is measured across the sheet thickness in different zones, and the mean value of hardness is calculated in each zone, wherein the maximum and minimum value of hardness is observed in the equiaxed grain zone and re-solidified zone respectively. The effect of laser power and sheet thickness on microhardness is also studied and it was observed that the hardness value has increased with the increase in laser power and decrease in sheet thickness.

v. A process map is generated with the application of the proposed analytical model for achieving defect-free bend during the laser forming process.

References

1. Chakraborty SS, Maji K, Racherla V, Nath AK (2015) Investigation on laser forming of stainless steel sheets under coupling mechanism. Opt Laser Technol 71:29–44. https://doi.org/10.1016/j.optlastec.2015.02.013
2. Maji K, Pratihar DK, Nath AK (2016) Experimental investigations, modeling, and optimization of multi-scan laser forming of AISI 304 stainless steel sheet. Int J Adv Manuf Technol 83:1441–1455. https://doi.org/10.1007/s00170-015-7675-0
3. Shen H, Vollertsen F (2009) Modelling of laser forming – an review. Comput Mater Sci 46:834–840. https://doi.org/10.1016/j.commatsci.2009.04.022
4. Shichun W, Jinsong Z (2001) An experimental study of laser bending for sheet metals. J Mater Process Technol 110:1999–2002
5. Marya M, Edwards GR (2002) An analytical model for the optimization of the laser bending of 124:6–13
6. Fetene BN, Kumar V, Dixit US, Echempati R (2018) Numerical and experimental study on multi-pass laser bending of AH36 steel strips. Opt Laser Technol 99:291–300. https://doi.org/10.1016/j.optlastec.2017.09.014
7. Kant R, Joshi SN (2016) Thermo-mechanical studies on bending mechanism, bend angle and edge effect during multi-scan laser bending of magnesium M1A alloy sheets. J Manuf Process 23:135–148. https://doi.org/10.1016/j.jmapro.2016.05.017
8. Yilbas BS, Akhtar SS (2014) Optics & Laser Technology Laser bending of metal sheet and thermal stress analysis. Opt Laser Technol 61:34–44. https://doi.org/10.1016/j.optlastec.2013.12.023
9. Kumar V, Dixit US (2017) Selection of process parameters in a single pass laser bending process. Engneering Optim 0273:1609–1624. https://doi.org/10.1080/0305215X.2017.1405395
10. Navarrete Á, Celentano D (2018) Effect of workpiece geometry using circular scan patterns in sheet laser forming processes. Int J Adv Manuf Technol 96:1835–1846. https://doi.org/10.1007/s00170-018-1628-3
11. Lambiase F, Di Ilio A, Paoletti A (2015) Optimization of multi-pass laser bending by means of soft computing techniques. Procedia CIRP 33:502–507. https://doi.org/10.1016/j.procir.2015.06.063
12. Roohi AH, Moslemi Naeini H, Hoseinpour Gollo M (2015) An experimental investigation of parameters effect on laser forming of Al6061-T6 sheets. Proc Inst Mech Eng Part L J Mater Des Appl 0:1–10. https://doi.org/10.1177/1464420715599181
13. Maji K, Pratihar DK, Nath AK (2013) Experimental investigations and statistical analysis of pulsed laser bending of AISI 304 stainless steel sheet. Opt Laser Technol 49:18–27. https://doi.org/10.1016/j.optlastec.2012.12.006
14. Shi Y, Shen H, Yao Z, Hu J (2007) Temperature gradient mechanism in laser forming of thin plates. Opt Laser Technol 39:858–863. https://doi.org/10.1016/j.optlastec.2005.12.006

15. Kyrsanidi AK, Kermanidis TB, Pantelakis SG (2000) An analytical model for the prediction of distortions caused by the laser forming process. J Mater Process Technol 104:94–102. https://doi.org/10.1016/S0924-0136(00)00520-3

16. Cheng PJ, Lin SC (2001) An analytical model to estimate angle formed by laser. J Mater Process Tech 108:314–319

17. Shen H, Shi Y, Yao Z, Hu J (2006) An analytical model for estimating deformation in laser forming. Comput Mater Sci 37:593–598. https://doi.org/10.1016/j.commatsci.2005.12.030

18. Lambiase F (2012) An analytical model for evaluation of bending angle in laser forming of metal sheets. J Mater Eng Perform 21:2044–2052. https://doi.org/10.1007/s11665-012-0163-x

19. Lambiase F, Di Ilio A (2013) A closed-form solution for thermal and deformation fields in laser bending process of different materials. Int J Adv Manuf Technol 69:849–861. https://doi.org/10.1007/s00170-013-5084-9

20. Eideh A, Dixit US, Echempati R (2015) Lasers based manufacturing. https://doi.org/10.1007/978-81-322-2352-8

21. Hu Y, Xie Y, Wu D, Yao Z (2019) Quantitative evaluation of specimen geometry effect on bending deformation of laser peen forming. Int J Mech Sci 150:404–410. https://doi.org/10.1016/j.ijmecsci.2018.10.040

22. Fetene BN, Shufen R, Dixit US (2018) FEM-based neural network modeling of laser-assisted bending. Neural Comput Appl 29:69–82. https://doi.org/10.1007/s00521-016-2544-9

23. Lambiase F, Di Ilio A, Paoletti A (2016) Productivity in multi-pass laser forming of thin AISI 304 stainless steel sheets. Int J Adv Manuf Technol 86:259–268. https://doi.org/10.1007/s00170-015-8150-7

24. Geiger M, Vollertsen F (1993) The Mechanisms of Laser Forming 42:301–304

25. Carslaw HS, Jaeger JC (1959) Conduction of Heat in Solids. Oxford University Press, USA

26. Ozisik MN (1993) Heat conduction. Wiley Intersci Publ. https://doi.org/10.1017/CBO9781107415324.004

27. Merklein M, Hennige MGT (2001) Laser forming of aluminium and aluminium alloys - microstructural investigation. J Mater Process Technol 115:159–165. https://doi.org/10.1016/S0924-0136(01)00759-2

28. Vollertsen F (1994) An analytical model for laser bending. Lasers Eng:261–276. https://doi.org/10.1243/PIME